

# OPTICAL, STRUCTURAL AND ELECTRICAL PROPERTIES OF SILAR DEPOSITED ZINC DOPED CADMIUM SULPHIDE THINFILMS

D. Pradhabhan\*<sup>1</sup> & Dr. A. Sakthivelu<sup>2</sup>

<sup>1,2</sup>PG & Research Department of Physics, Periyar E.V.R College, Trichy, Tamilnadu.

Received: February 03, 2019

Accepted: March 25, 2019

**ABSTRACT** The Zn doped CdS thin films were prepared on well cleaned glass substrates by SILAR deposition technique using cadmium acetate, zinc acetate and thiourea as precursor solution with deposition cycles of 75 dippings for various (3, 6 and 9) Zn mol%. The prepared samples were annealed in air. The prepared thin films were characterized for their structural, micro structural and optical properties by XRD, FESEM and UV-Visible spectroscopy. The XRD analysis shows that, the prepared samples are polycrystalline and it exhibits cubic structure. The morphology of the Zn doped CdS thin films characterized by FESEM revealed that the film consisted of mixture of nanoparticles and the EDAX results showed the presence of Zn and CdS in the prepared thin films. The optical properties of the deposited films were characterized by UV-VIS. Optical band gap was blue shifted with increase in Zn doping which is associated with Moss-Burstein (MB) effect. The electrical properties of the CdS thin films characterized by Hall measurements. It is observed that, for increase in Zn doping concentration, the resistivity decreases, conductivity and Hall mobility increases with Zn doping concentration. CdS film coated with 6 mol % Zn concentration had higher carrier concentration, conductivity and lower resistivity than other two samples.

**Key Words:** SILAR, Zn doped CdS thin films, XRD, surface morphology, Electrical properties.

## 1. Introduction

Now day solar cell devices play vital role in converting solar energy into usable form. The science and technology of photovoltaic devices (solar cells) and systems have undergone revolutionary developments. Many type of thin film solar cells exists today; the major contributors being crystalline silicon, amorphous crystalline gallium-arsenide, poly-crystalline copper-indium gallium diselenide (CuIGS) and polycrystalline cadmium telluride (CdTe)[1-8]. In the past few years, II-IV semiconductors thin films have attracted considerable attention from the research community because of their wide range of applications in the fabrication of solar cells and other electronic and opto-electronics devices. Cadmium (CdS) is mostly used as a window layer for photo voltaic devices. Cadmium sulphide (CdS) is an important n-type semiconductor with a low direct band gap used as window layer material in solar cell devices. CdS absorbs blue portion of solar radiations and decrease the current density of solar cells. Doping with Zn to CdS window material improves the electrical and optical properties of thin films. The Zn doped CdS provides the wider band gap and higher optical transmittance as compared to CdS. The efficiency of solar cell devices is found to be enhanced by increasing the band gap of buffer layer. Out of available thin film deposition technique, the most simple and non-vacuum technique Successive Ionic Layer Adsorption and Reaction (SILAR) [10, 11] is implemented in present work. It is a low cost and always proffered for larger surface area deposition. The present study aims with deposition of  $Cd_xZn_{1-x}S$  thin films by using Successive Ionic Layer Adsorption and Reaction (SILAR).

## 2. Experimental

All the chemicals used for the thin films preparation were of analytical grade. It includes cadmium acetate, thiourea and zinc acetate. All the solutions were prepared in double distilled water. For the preparation of Zn doped CdS thin films, cationic precursor (0.1M) cadmium acetate (50 ml) and (0.003 M) aluminium nitrate were taken in a beaker, and the anionic precursor (0.1M) thiourea (50 ml) was taken in a separate beaker. For the deposition of Zn doped CdS thin film, well cleaned glass substrate was dipped into the cationic precursor for 40 sec for adsorption of  $Cd^{2+}$  and  $Zn^{2+}$  ions on the surface of the glass substrate, and then the substrate was dipped into the de-ionized water for 10 sec to avoid precipitation and also to remove the loosely bounded cations. The substrate was then immersed into the anionic precursor bath ( $S^{2-}$ ) for 40 sec. The procedure was carried out at  $\sim 75^\circ C$  temperature. Successive dipping cycles repeated up to 75 cycles, to get the well adherent and homogeneous Zn doped CdS thin films. Then the same procedures were repeated for 0.006M and 0.009 M zinc acetate. Zn was doped with CdS in the

following mol % and they are 3, 6 and 9 respectively. The prepared samples were annealed in air at 200°C for 1 hour. Phase identification and crystalline properties of the films were studied by XPERT-PRO X-ray powder diffractometer with CuK $\alpha$  radiation ( $\lambda = 1.5418\text{\AA}$ ). Scanning electron microscopy FE-SEM 6701 F used to study the surface morphology and to illustrate the formation of crystallites on the film surface. UV-VIS spectrophotometric measurements were performed using a Unico UV-2102PCS spectrophotometer at room temperature.

### 3. Results and Discussion

#### 3.1. UV Visible spectroscopy

The optical properties of thin films such as transmission, refractive index and energy gap are of great importance to identify their suitability as window layer material for solar cell applications. The transmittance spectra of Zn-doped CdS thin films are shown in Figure 3.1.1 The transmittance increases with increasing Zn concentration, which may be attributed to the lesser crystallite size of these films as observed from the XRD analysis (Table 3.2.1). It is well known that when the crystallite size is small, the smoothness of the film increases which cause an enhancement in the optical transmittance. The higher transmittance indicates lower defect density and better electrical properties of the doped CdS films because absorption of light in the longer wavelength region (>500 nm) is usually caused by crystalline defects such as grain boundaries and dislocations [12]. Furthermore, from the absorption spectra, the optical band gap energy  $E_g$  of the Zn-doped CdS thin films was calculated using the dependence of the absorption coefficient ( $\alpha$ ) on the photon energy ( $h\nu$ ) [19]:

$$\alpha h\nu = A (h\nu - E_g)^{1/2} \quad (1)$$

Figure 3.1.2 shows the plot of  $(\alpha h\nu)^2$  vs.  $(h\nu)$  for the undoped and Zn-doped CdS thin films. Extrapolation of the linear portion of the plot onto the energy axis gives the band gap values of the films.

The  $E_g$  value increases gradually as the Zn doping level increases and attains a maximum value of 2.66 eV for the CdS film doped with 6 mol.% Zn concentration. Beyond this doping concentration, the band gap decreases to 2.5 eV for the CdS film coated with 9 mol.% Zn concentration. This variation in  $E_g$  is associated with the Moss-Burstein (MB) effect or band gap widening (BGW) mechanism [13]. According to Moss – Burstein effect, the optical absorption edge of a degenerate n-type semiconductor is shifted towards higher energy by an amount proportional to the electron density in the conduction band. From theoretical calculations, Zaoui et al. [14] proposed that the optical band gap of Zn-doped CdO films increases if Zn<sup>2+</sup> ions successfully replace Cd<sup>2+</sup> ions in the CdO lattice. The increased band gap values observed here confirms that Zn<sup>2+</sup> ions successfully replace Cd<sup>2+</sup> ions in the CdS lattice. Increased band gap values observed for the Zn doped CdS films might be due to decreased crystallite size values which lead to quantum confinement of the charge carriers in the crystallites and this result in the reduction of band bending effect, the degree of preferred orientation, and stoichiometry [15]. In nanocrystalline materials, band bending effect can be expected at the grain boundaries as the surface to volume ratio is higher. Normally, in crystallites with smaller size, the band bending effect will be more compared to bigger crystallites. Owing to quantum confinement, the band gap increases due to reduced crystallite size, which result in the shift of absorption threshold to shorter wavelength due to individual confinement of electrons and holes. The energy gap broadening may also be related to the existence within the band gap of a high density levels with energies near the bands, which can give rise to band tailing as has been suggested for many polycrystalline materials. This is in accordance with the results reported by Rajashree et al. [16] for Cd-doped PbS thin films. The wide band gap and high optical transparency observed for the Zn doped CdS films make them possible window layers in solar cell applications.

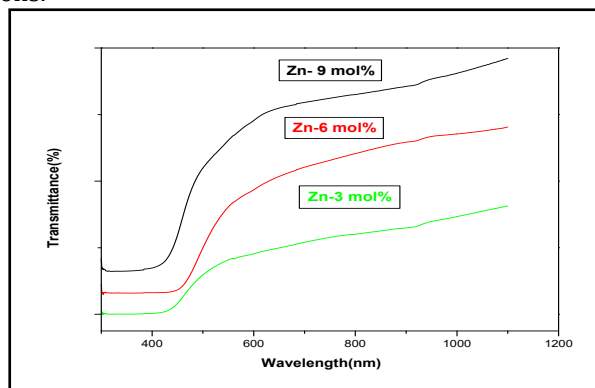


Figure 3.1.1 –The transmittance spectra of Zn-doped CdS thin films

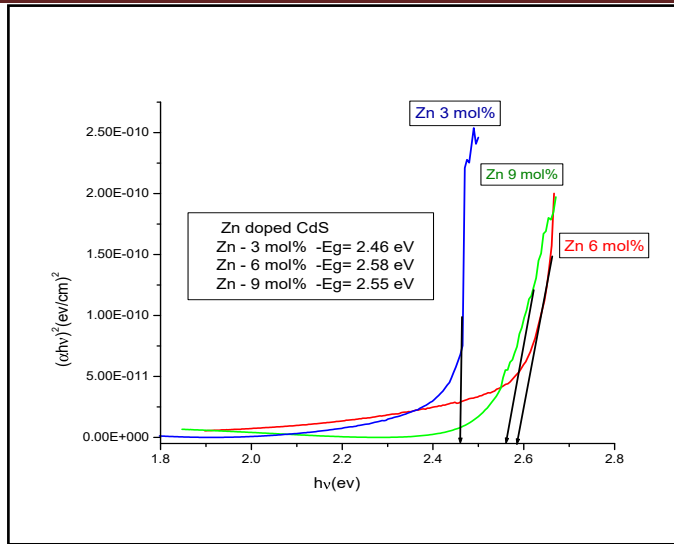


Figure 3.1.2 shows the plot of  $(\alpha hv)^2$  vs.  $(hv)$  for the undoped and Zn-doped CdS thin films.

### 3.2. XRD Analysis

The X-ray diffraction (XRD) patterns of the Zn-doped SILAR deposited CdS films are shown in Fig.3.2.1.

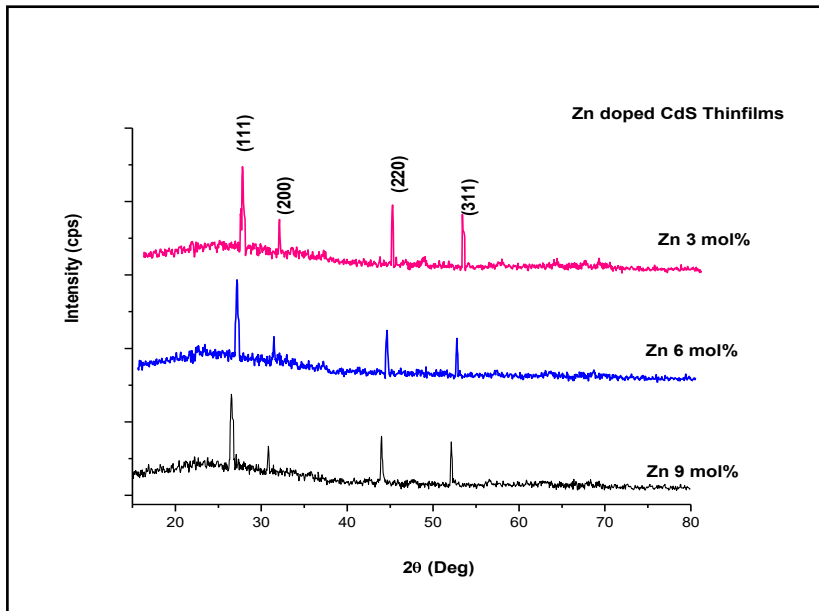


Fig.3.2.1 - XRD patterns of the Zn-doped CdS films for various Zn doping concentration.

The diffraction peaks reveal that the films show a polycrystalline nature of cubic (zinblende) [ICDD No. 10-0454] phase, with a (1 1 1) preferred orientation, irrespective of the Zn doping level, indicating that the incorporation of Zn into the Cd sites does not alter the preferential growth. No peaks related to ZnS are observed in the patterns, indicating the purity of the films. The variation of the preferential orientation factor  $f(1\ 1\ 1)$  as a function of Zn doping level is presented in Table 3.2.1.

Zn doping concentration (Mol. %)	2θ position for the (111) plane	Preferential orientation factor for f(111)	Crystallite size, D (nm)	Lattice parameters* (Å)		c/a
				'a'	'c'	
3	26.542	0.53	20.93	4.1096	6.711	1.633
6	26.602	0.50	17.49	4.1005	6.696	1.6329
9	26.610	0.46	16.66	4.0883	6.694	1.6329

Table .3.2.1 - Observed 2θ values and structural parameters of Zn-doped CdS thin films

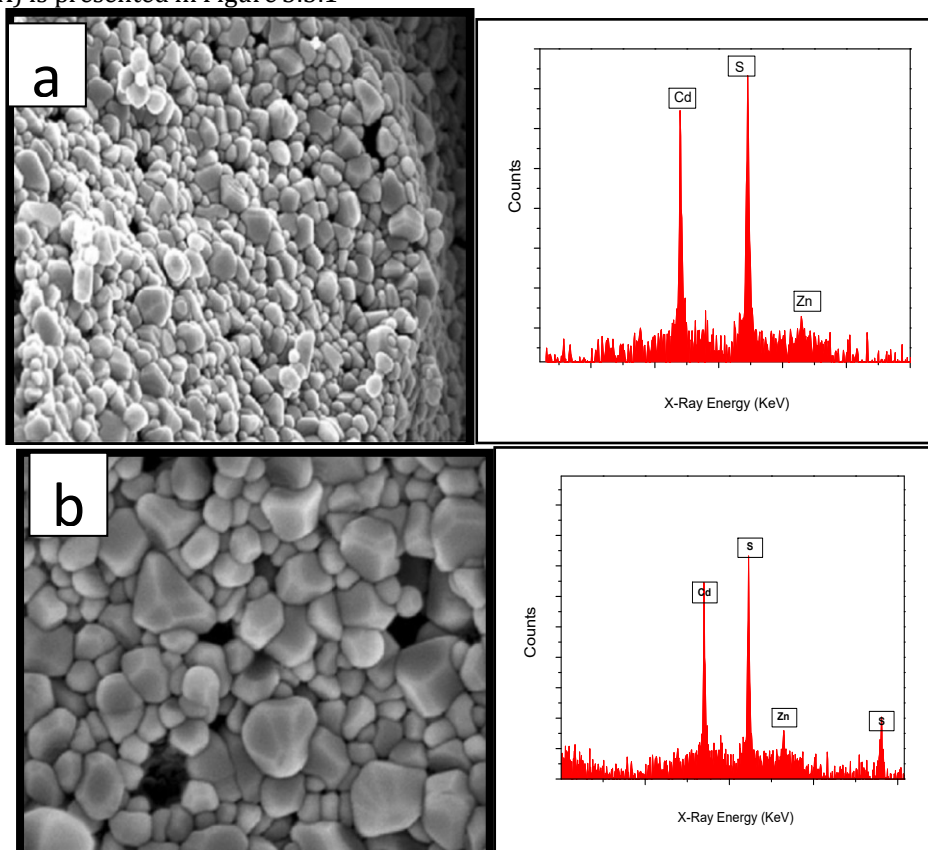
As seen from Table 3.2.1,  $f(1\ 1\ 1)$  decreases up to 6 mol %Zn doping concentration and then it increases for further Zn doping, suggesting a monotonical deterioration in the crystalline quality due to Zn doping. There are several possibilities by which  $Zn^{2+}$  ions may be incorporated into the host CdS crystalline structure,  $Zn^{2+}$  ions may occupy interstitial positions in the CdS lattice, occupy empty locations of  $Cd^{2+}$  ions or substitutionally replace  $Cd^{2+}$  ions. The low value of  $f(1\ 1\ 1)$  obtained for the films up to 6 mol %Zn doping might be due to the structural disorder introduced in the system due to the interstitially occupied  $Zn^{2+}$  ions. Above 6 at % Zn doping concentration,  $Zn^{2+}$  ions enters the lattice both substitutionally and interstitially and as a result the  $f(1\ 1\ 1)$  value slightly increases. The small reduction of the lattice parameters observed for Zn doped CdS films (Table 3.2.1) can be a consequence of the incorporation of Zn into the lattice. The ionic radii mismatch between  $Cd^{2+}$  and  $Zn^{2+}$  can be the cause for the reduction of lattice parameters of the doped films. This supposition can be happen if the zinc ions enter substitutionally Cd sites. A small shift in the  $(1\ 1\ 1)$  diffraction peak towards a high diffraction angle indicates the contraction in the CdS films with Zn doping. The  $c/a$  ratio is found to be almost constant inferring that doping does not affect the fundamental structure of the undoped system i.e., 'Zn' ion occupies the 'Cd' (metallic) site in the host lattice. The 'a' and 'c' values decreases with doping, keeping  $c/a$  constant. The crystallite sizes (D) of the Zn doped CdS films was calculated by using the Scherrer relation [17]:

$$D = 0.9 \lambda / \beta \cos \theta \quad \text{-----} \quad (1)$$

where  $\beta$  is the full width at half maximum (FWHM),  $\lambda$  is the wavelength of the X-ray ( $1.5406 \text{ \AA}$ ) and  $\theta$  is the angle of diffraction. The crystallite size decreases gradually as the Zn doping level in the Zn doping concentration increases and attains a minimum value of 16.66 nm. This decrease in crystallite size may be caused by the enhanced incorporation of  $Zn^{2+}$  ions into the  $Cd^{2+}$  sites.

### 3.3. Surface Morphology and EDAX by FESEM Analysis

Field Emission Scanning Electron Microscope (FESEM) is very helpful to study the surface morphology of thin films. Figure 3.3.1 shows the FESEM image of the Zn doped CdS thin films. It is observed that Zn doped CdS thin films are homogeneous and uniformly spread on the substrates. It can be seen that all the particles were in more or less spherical shape with a wide particle size distribution with well separated grain boundaries. The FESEM image shows the compact polycrystalline surface composed of a single type of small, densely packed nanosized grains uniformly distributed over smooth homogeneous background. The quantitative compositional analysis of the CdS film made using energy dispersive X-ray analysis (EDX) is presented in Figure 3.3.1



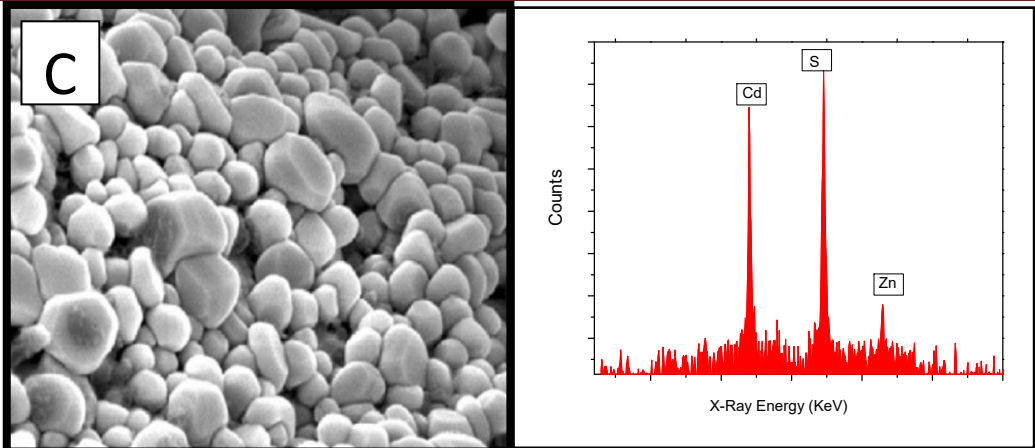


Figure 3.3.1 - FESEM and EDAX images of the Zn doped CdS thin films (a - Zn 3 mol%, b - Zn6 mol%, c - Zn 9 mol%).

### 3.4 Electrical studies

Figure 3.4.1 shows the variation of resistivity and conductivity of Zn doped CdS films as a function of Zn concentration.

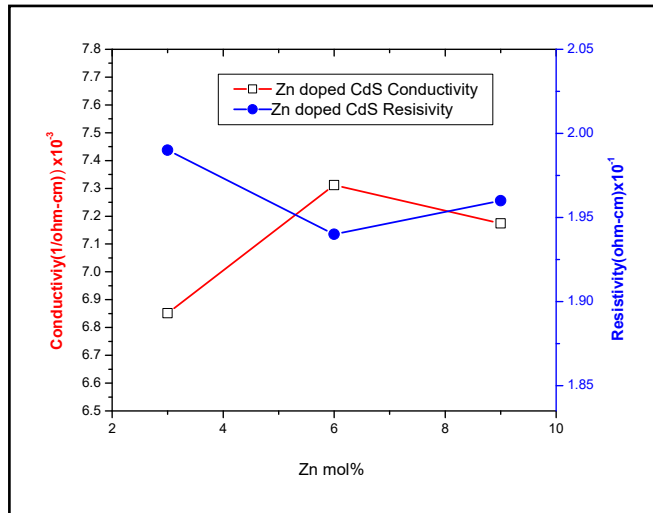


Figure 3.4.1 - The variation of resistivity and conductivity of Zn doped CdS films as a function of Zn doping concentration.

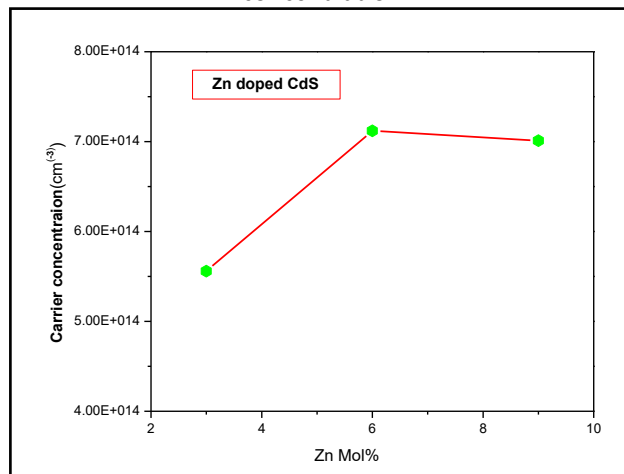


Figure 3.4.2 - Variations of carrier concentration of Zn doped CdS thin films as a function of Zn doping concentration.

Zn doping %	Resistivity ( $\Omega \cdot \text{cm}$ )	Mobility ( $\text{cm}^2/\text{Vs}$ )	Carrier concentration ( $\text{cm}^{-3}$ )	Hall coefficient ( $\text{cm}^3/\text{coul.}$ )	Conductivity ( $1/\text{ohm}\cdot\text{cm}$ )
3	$1.99 \times 10^{-1}$	$7.21 \times 10^3$	$5.56 \times 10^{14}$	$3.70 \times 10^3$	$6.851 \times 10^{-03}$
6	$1.94 \times 10^{-1}$	$8.34 \times 10^3$	$7.12 \times 10^{14}$	$4.14 \times 10^4$	$7.312 \times 10^{-03}$
9	$1.96 \times 10^{-1}$	$8.46 \times 10^3$	$7.01 \times 10^{14}$	$4.63 \times 10^4$	$7.174 \times 10^{-03}$

Table.3.4.1 – Resistivity, conductivity and carrier concentrations of Zn doped CdS thin films

As seen in Figure 3.4.1, the resistivity decreases with increasing Zn doping concentration in the films up to 6 mol.%, after which it slightly increases. The decreases in resistivity up to 6 mol % Zn concentrations might be due to the increase in the carrier concentration of the doped films due to the substitutional replacement of  $\text{Cd}^{2+}$  ions by  $\text{Zn}^{2+}$  ions. Flores et al [18] also reported a similar behaviour for fluorine doped CdS thin films. They quoted that the free carrier concentration increases due to substitutional incorporation of F- ions in the CdS structure which results in the decreased resistivity of the films. DeMelo et al [19] quoted sulphur deficiencies contribute to the increase in free carrier concentration of the films, which reduces the resistivity of the films. Although the crystalline quality of CdS film slightly decreases with Zn doping increased sulphur vacancies might have played an important role in improving its electrical properties.

### Conclusions

Zn doped CdS nano crystalline thin films for various (3, 6, 9) mol % have been prepared by SILAR method using cadmium acetate, zinc acetate and thiourea. The XRD pattern reveals that Zn doped CdS thin films contain the mixture of cubic phase nanoparticles of size 16-20 nm. The intensity peaks indicate that synthesized product is crystalline and pure. The result of UV-Vis. spectrum shows that The  $E_g$  value of prepared Zn doped CdS thin film is increases gradually as the Zn doping level increases and attains a maximum value of 2.66 eV for the CdS film doped with 6 mol. % Zn concentrations. Beyond this doping concentration, the band gap decreases to 2.5 eV for the CdS film coated with 9 mol.% Zn concentration. FESEM micrograph witnesses all the particles were in more or less spherical shape with a wide particle size distribution with well separated grain boundaries. The FESEM image shows the compact polycrystalline surface composed of a single type of small, densely packed nanosized grains uniformly distributed over smooth homogeneous background. EDAX analyses of the prepared Zn doped CdS thin films confirm that the samples are composed of Cd, Zn and S without any impurity. From the Hall measurements, it is observed that, the resistivity of the prepared samples decreases with increasing Zn doping concentration in the films up to 6 mol.%, after which it slightly increases. The decreases in resistivity up to 6 mol % Zn concentrations might be due to the increase in the carrier concentration of the doped films due to the substitutional replacement of  $\text{Cd}^{2+}$  ions by  $\text{Zn}^{2+}$  ions.

### References

- [1] Huan Ke, et al, "Effect of temperature on structural and optical properties of ZnS thin films by chemical bath deposition without stirring the reaction bath," *Materials Science in Semiconductor Processing*, vol. 18, pp. 28-35, 2014.
- [2] Jung Hoon Ahn, Kwun Nam Hui, Kwan San Hui, Young Guk Son, and Dong Hyun Hwang, "Structural and optical properties of ZnS thin films deposited by RF magnetron sputtering," *Nanoscale Research Letters*, vol.7(2), 2012.
- [3] Raghad Zein, and Ibrahim Alghoraibi, "Effect of Deposition Time on Structural and Optical Properties of ZnS Nanoparticles Thin Films Prepared by CBD Method ," *International Journal of Chem. Tech Research CODEN (USA)*, vol.6(5), pp. 3220-3227, 2014.
- [4] Nada K. Abbas, Lamia K. Abbas, and Suaad A-Muhammed, "Effect Of Thickness on Structural and Optical Properties of  $\text{Zn}_x\text{Cd}_{1-x}\text{S}$  Thin Films prepared by Chemical Spray Pyrolysis," *Int. J. Thin Film Sci.*, vol. 2 (2), pp. 127-132, 2013.
- [5] T.O. Berestok, D.I. Kurbatov, N.M. Opanasyuk, A.D. Pogrebnyak, O.P. Manzhos1, and S.M. Danilchenko, "Structural Properties of ZnO Thin Films Obtained by Chemical Bath Deposition Technique," *J. of Nano and Elect. Phy* vol. 5(1), 2013.
- [6] W. Wang, I. Germanenko, and M. Samy El-Shall, "Room Temperature Synthesis and Characterization of Nanocrystalline CdS, ZnS, and  $\text{Cd}_x\text{Zn}_{1-x}\text{S}$ ," *Chemistry of Materials*, vol. 14(7), pp. 3028-3033, 2002.
- [7] S. Ilican, Y. Caglar and M. Caglar, "Effect of the Substrate Temperatures on the Optical Properties of the Cd 0.22 Zn0.78S Thin Films by Spray Pyrolysis Method," *Physica Macedonica*, vol. 56, pp. 43- 48, 2006.
- [8] Jie Cheng, DongBo Fan, Hao Wang, BingWei Liu, YongCai Zhang, and Hui Yan, "Chemical bath deposition of crystalline ZnS thin films," *Semiconductor Science and Technology*, vol.18, (7), 2003.
- [9] R.Radha, A.Sakthivelu, D.Pradhban, C.Ravichandiran, S.Murugesan, E.Mohandas and Geethadhevi, *International Journal of ChemTech Research*, Vol.6, No.6, pp 3374-3377(2014)
- [10] R. Radha, A. Sakthivelu, D.Pradhban, C. Ravichandiran, S. Murugesan, & E. Mohandas, *Journal of Scientific Research in Physical & Mathematical Science* Volume (2) Issue (9) Year (2015)ISSN : 2349-7149
- [12] M. Cao, L. Li, B.L. Zhang, J. Huang, H. Cao, Y. Sun, Y. Shen, Influence of substrates on the structural and optical properties of ammonia-free chemically deposited CdS films, *J. Alloys Compnds.* **530**(2012) 81–87.

- [13] E. Burstein, Anomalous optical absorption limit in InSb, *Physical Review* **93**(1954) 632–633.
- [14] A. Zaoui, M. Zaoui, S. Kacimi, A. Boukourt, B. Bouhafs, Stability and electronic properties of ZnxCd1-xO alloys, *Mater. Chem. Phys.* **120**(2010) 98–103.
- [15] J.P. Enriquez, X. Mathew, Influence of the thickness on structural, optical and electrical properties of chemical bath deposited CdS thin films, *Sol. Energy Mater. Sol. Cells*, **76**(2003) 313–322.
- [16] C. Rajashree, A.R. Balu, V.S. Nagarethinam, Properties of Cd-doped PbS thin films: Doping concentration effect, *Surf. Engg.* **31**(2015) 316–321.
- [17] S Tewari and A Bhattacharjee, *Pramana – J. Phys.* **76**, 153 (2011)
- [18] F.de Moure-Flores, K.E. Nieto-Zepeda, A. Guillen -Cervantes, S. Gallando, J.G. Quinones-Galvan, A. Hernandez-Hernandez, M.de la L.Olvera, M.Zapata- Torres, Yu Kundriavtsev, M.Melendez-Lira, Effect of the immersion in CdCl<sub>2</sub> and annealing on physical properties of CdS:F films grown by CBD, *J. Phy. Chem. Solids*, **74**(2013) 611–615.
- [19] O. De Melo, L. Hernandez, O. Zelaya-Angel, R. Lozada-Morales, M. Becerril, E. Vasco, Low resistivity cubic phase CdS films by chemical bath deposition technique, *Appl-phys.Lett.* **65**(1994) 1278–1280.